International Journal of Innovative Research in Engineering and Management (IJIREM)
ISSN (Online): 2350-0557, Volume 13, Issue 3, June 2026
DOI: https://doi.org/10.55524/ijirem.2026.13.3.18
Article ID IJIR3220, Pages 153-163
www.ijirem.org

Experimental Study on Punching Shear Performance of Two-Layer Normal and Steel Fiber Reinforced Concrete Slabs

Hawkar Azeez Ahmed[1], and Esra Mete Güneyisi[2]

[1, 2] Department of Civil Engineering, Gaziantep University, 27310, Gaziantep, Türkiye

Correspondence should be addressed to Hawkar Azeez Ahmed hawkar.ahmed01@outlook.com

Received: 3 June 2026; Revised: 17 June 2026; Accepted: 30 June 2026

ABSTRACT- This study experimentally investigates the punching shear response of two-layer slabs having normal concrete (NC) with steel fiber reinforced concrete (SFRC). The concept of the two-layer system is simple: fibers are only cast in the areas where the critical cracks are likely to occur, thus minimizing the amount of the more costly fibered concrete. A total of 15 flat-slab specimens were cast and divided into five parametric groups, with a normal concrete slab as the reference slab, and the other slabs having different variables such as the fiber height ratio through the slab depth, the flexural reinforcement ratio, the lateral size of the SFRC zone around the column, the load eccentricity, and the fiber volume fraction. Each specimen was loaded to failure and the response was monitored using load-deflection curves, cracking and ultimate loads, steel and concrete strains, punching cone geometry, ductility, and secant stiffness. The measured capacities were then compared with the ACI 318 punching provisions. The results indicated that the through-depth location of the fibers is an independent design variable, that the fibered zone is effective only if it is sufficiently thick to intersect the incipient failure surface, and that the dosage of fibers increases both the cracking load and the ultimate load. However, most of the fibre benefit was negated by load eccentricity which also altered the mode of failure. However, ACI predictions were conservative for each concentric specimen, and did not consider the contribution of the fibers, the zone-size effect, or the eccentric failure mode.

KEYWORDS- Flat Slab; Punching Shear; Slab-column Connection; Steel Fiber Reinforced Concrete; Two-layer Slab.

I. INTRODUCTION

In the field of building construction, reinforced concrete slab-column floors such as flat slabs are widely used in construction as they do not require deep beams, are easy to form, and can reduce the story height [1], [2]. This is because the gravity load is transferred directly from the slab to the column, which makes the design of the floor easier, but puts a heavy load on the connection area. Punching shear is the most important local failure. It is when high forces are applied to the column, resulting in high shear stresses and cracking at the point of application, and the slab then cracks around the column in a punching cone. The main concern regarding this failure is in its characteristics as it can occur without a warning and can lead to sudden and brittle progressive collapse [2], [3].

The prediction of punching capacity is not straightforward, as it is influenced by a number of interacting material and geometric parameters, and because the design codes do not consider the same parameters. The capacities of each code are based on different theoretical models or empirical formulations and can result in different capacities for the same connection [1], [3], [4]. A set of common parameters are identified as the main parameters that affect strength and deformation for all experimental programs, such as concrete strength, flexural reinforcement ratio, column size and slab slenderness [4], [5]. The flexural reinforcement ratio is particularly significant as it affects flexural capacity and stiffness, and thus rotation and crack width in the vicinity of the column. For lightly loaded buildings, slabs with low reinforcement ratios can have extensive yielding before punching, which can alter the failure mode of the slab to a flexure-influenced failure [5].

Due to its brittle and critical nature, a variety of punching strengthening methods have been investigated [2]. Transverse shear reinforcement in the form of stirrups or studs intercepts the inclined cracking and provides load paths after cracking, and it has been demonstrated to increase punching capacity and enhance ductility [1], [6]. The downside is that it can take up a lot of space in the connection area and may be more difficult to detail. Material-based strengthening strategies are considered when space is an issue in the strengthening process. Tremendous research has been conducted on the use of steel fiber reinforced concrete due to its capacity to target the governing mechanism behind shear transfer. The fibers help bridge the crack faces and spread the tensile stress over the crack leading to reduced spacing of the cracks and enhancing the punching resistance capacity as well as increased ductility [7].

Most of the up-to-date studies have concerned monolithic slabs in different configurations including plain reinforced concrete and single layer steel fiber reinforced concrete. No studies have investigated two-layered plain and steel fiber reinforced concrete slabs' response to punching, which is a critical gap in the literature since the critical shear crack and the rotation profile could interact with the position of the fibers relative to the tension and compression zones, and with the interface between the two layers [8]. The present research aims to fill this gap by exploring the punching capacity of two-layered slabs cast in normal concrete and steel fiber reinforced concrete and investigates the cracking behavior and deformation response in the slabs and compares the findings with ACI 318 predictions.

II. EXPERIMENTAL PROGRAM

A. Materials and Mix Proportions

All materials used were ordinary Portland cement, natural sand and crushed coarse aggregate within the ASTM C33 limits. A polycarboxylate ether based high-range water reducer was added to enhance workability. The target compressive strength of 25 MPa was set for the plain normal concrete, and a series of trial batches were prepared by adjusting the cement content, aggregate proportions, water-to-cement ratio, and dosage of admixtures to obtain a suitable mix. The selected reference mix is summarized in Table 1. The SFRC series was then prepared with the same base proportions without any changes. The hooked-end steel fibers were not used to replace any ingredient in the reference mix but were simply added to the reference mix as an additional constituent, as was the case with the admixture. The fibers took up some of the batch volume, so the paste and aggregate phases were slightly reduced, and this was controlled during mixing by adding the fibers towards the end of the mixing cycle, which reduced the workability of the mix.

Table 1: Reference concrete mix proportions and hooked-end steel fiber properties

Mix constituent	Quantity	Steel fiber property / value
Cement	290 kg/m³	Type: Hooked-end
Fine aggregate	939 kg/m³	Length: 25 mm
Coarse aggregate	918 kg/m³	Diameter: 0.25 mm
Water	188.5 kg/m³	Aspect ratio: 100
Water-to-cement ratio	0.65	Tensile strength: 2850 MPa
Superplasticizer	1.45 kg/m³	Elastic modulus: 200 GPa
28-day mean strength	25.07 MPa	Density: 7900 kg/m³

B. Specimen Geometry and Test Matrix

Figure 1 presents the slab and column dimensions used in the research. As shown in the figure, the slabs were cast 650 mm by 650 mm and had a thickness of 60 mm. The column centered on the slabs was cast 120 mm by 120 mm with a height of 150 mm. It is also shown that the slabs' clear span was 600 mm by 600 mm leaving a 25 mm overhang beyond the supports.

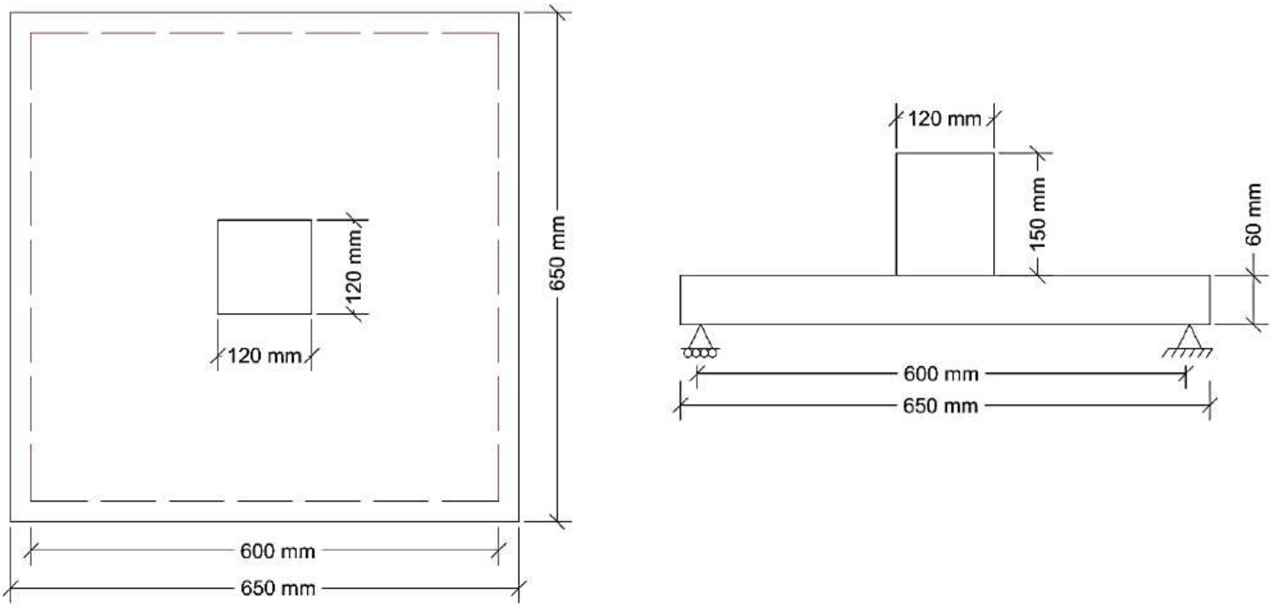

Figure 1: Slab dimensions and specimen geometry.

The program comprised fifteen specimens in five parametric groups, each of which differed by one parameter while the remaining parameters were kept constant as shown in Figure 2. The reference for all groups was the plain normal concrete slab S1, which was cast without fibers at a flexural reinforcement ratio of 1.346%. Groups 1, 2, 4 and 5 used the same common SFRC reference (Specimen S2) and are referred to as S6/S2, S10/S2 and S14/S2. Group 1 varied the ratio of the height of the fiber with depth (S1: 0, S2: SFRC in the lower half, S3: cast full-depth in SFRC). Group 2 changed the flexural reinforcement ratio from 0.725 to 1.035 and 1.346 percent. In Group 3, the lateral dimension of the fibered zone around the column was varied to C+d, C+2d and C+3d. Group 4 changed the load eccentricity (e = 0, 60, 120 mm) and Group 5 changed the fiber volume fraction (0.5, 1.0, 1.5 percent).

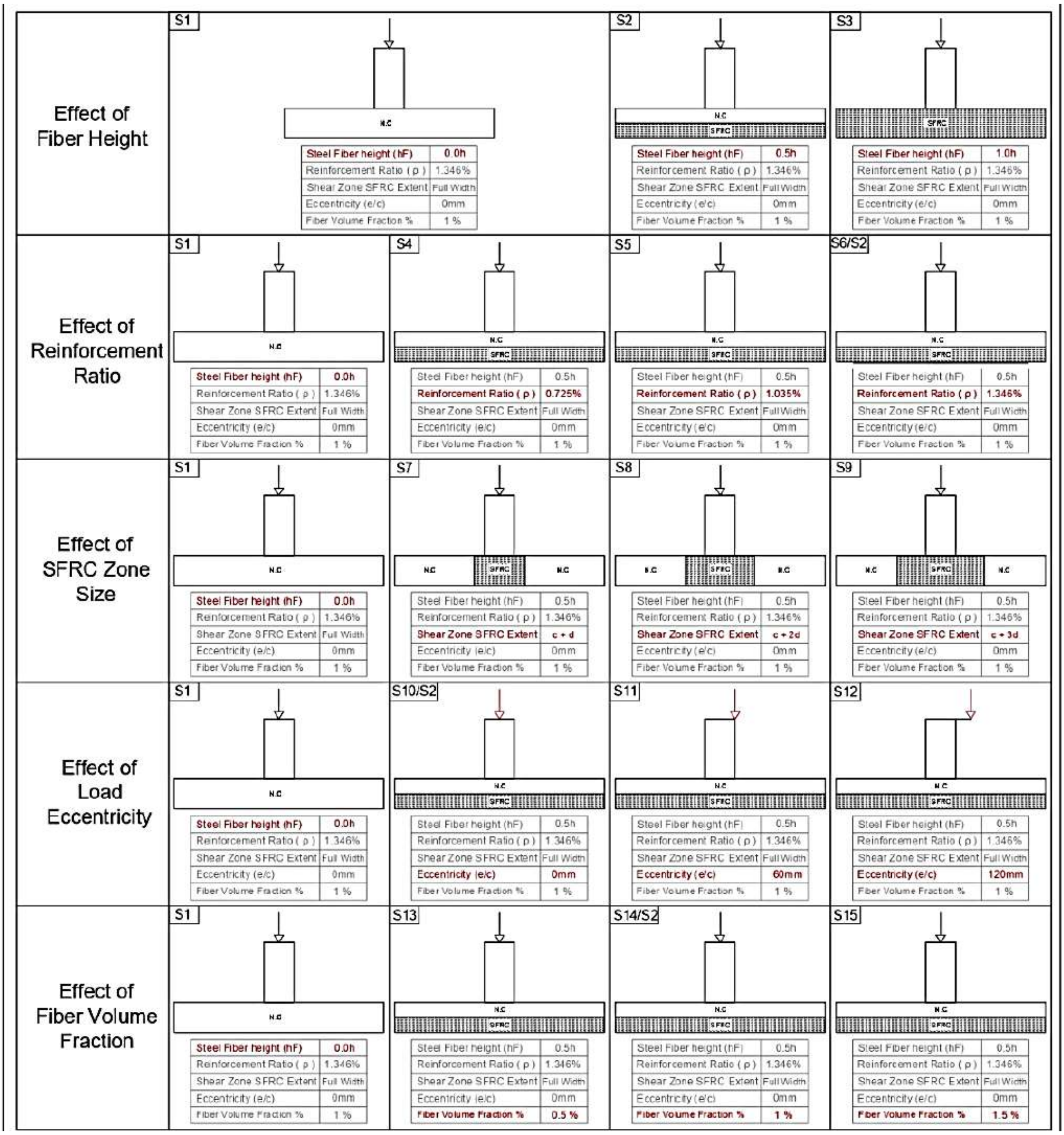

Figure 2: Testing program and full specimen matrix for the five parametric groups.

C. Instrumentation and Test Procedure

A centrally applied load through the column stub was used to load each slab to failure, while the eccentric specimens were loaded at the offsets shown above. A load cell was used to measure the load and the deformation response was measured at several locations. The central deflection was measured using linear transducers. Electrical resistance strain gauges were placed on the main tension reinforcement at a distance d from the face of the column and on the slab soffit in the longitudinal, diagonal and front directions to measure the strains of the steel and concrete at first crack and at ultimate. The punching cone was traced from the post-test photographs in AutoCAD and the cone area, perimeter and failure angles were measured for each specimen.

III. RESULTS AND DISCUSSION

The plain reference slab S1 failed in a typical brittle punching mode with a well-defined circumferential crack around the column, limited radial cracking on the tension face and small deformation before failure. The specimens with SFRC reacted differently and cracking took longer and spread over a wider area, deflected more, and in most cases carried a higher ultimate load. This behavior confirms the role of fibers, as their use led to changing the crack and damage paths and bridged the first cracks upon forming and allowed the slab to resist longer along with the increased load compared to the slabs cast in plain concrete, and this finding is consistent with the findings of other researchers [9], [2], [7].

A. Effect of Fiber Height Ratio (Group 1)

The plain reference slab S1 failed in a typical brittle punching mode with a well-defined circumferential crack around the column, limited radial cracking on the tension face and small deformation before failure. The specimens with SFRC reacted differently and cracking took longer and spread over a wider area, deflected more, and in most cases carried a higher ultimate load. This behavior confirms the role of fibers because the use of fibers resulted in changing the crack and damage paths and the slab resisted longer with the increased load compared to the slabs cast in plain concrete, and this finding is consistent with the findings of other researchers [9], [2], [7].

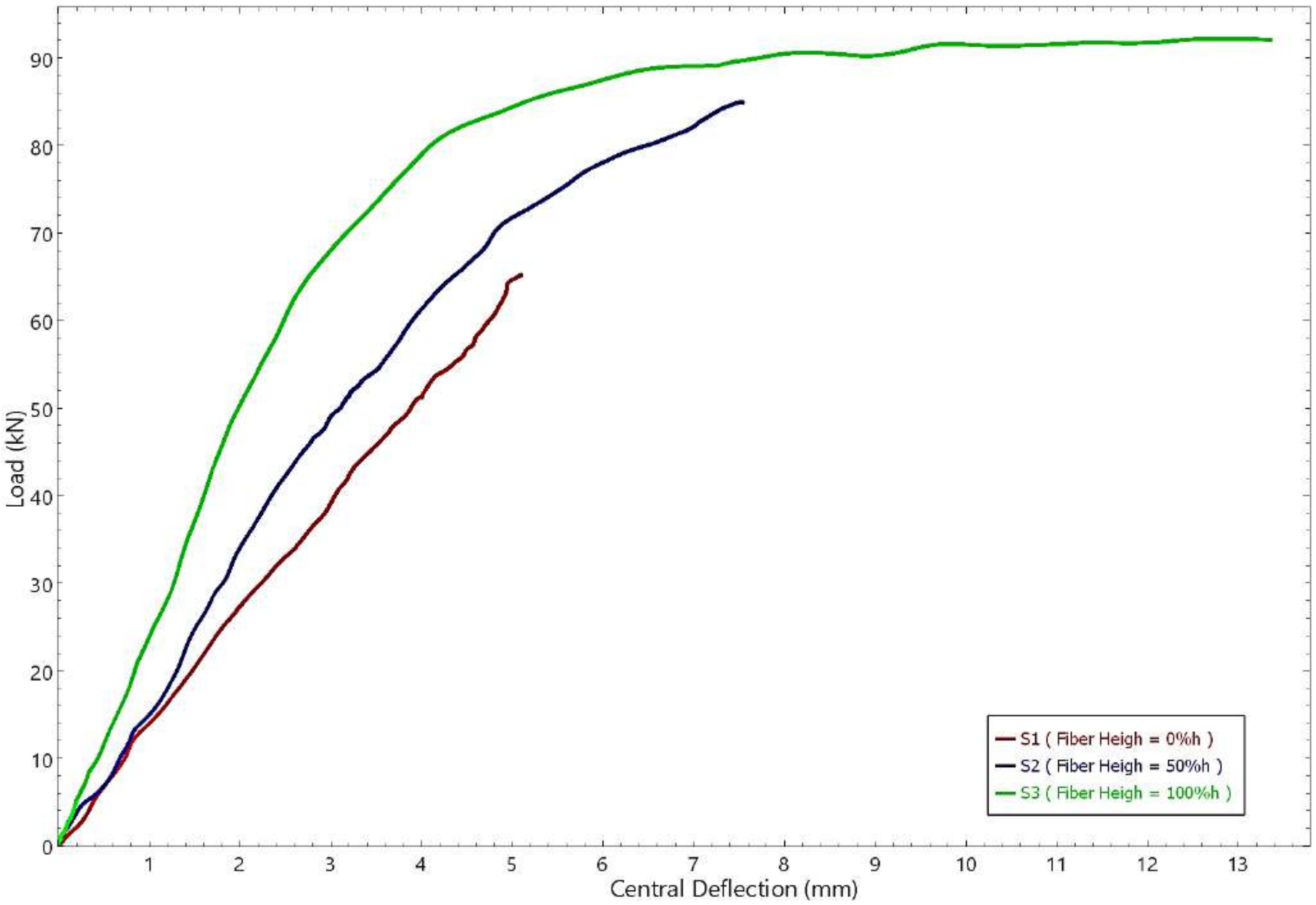

Figure 3: Load versus central deflection, Group 1 (effect of fiber height ratio).

Table 2: Critical loads and central deflections, Group 1 (effect of fiber height ratio)

Slab	Stage	Load (kN)	Central deflection (mm)
S1	First crack	25.00	1.82
S1	Ultimate	65.11	5.10
S2	First crack	46.00	2.77
S2	Ultimate	85.19	7.53
S3	First crack	58.00	3.25
S3	Ultimate	95.16	13.36

The flexural cracking begins at the bottom of the section under this loading, and the benefit of the bridging action is greatest in this area, with the tension half already providing a significant portion of the benefit. The extra advantage of the full-depth specimen is a result of the geometry of the punching mechanism itself. If the whole depth is fibered, the inclined crack will go through a bigger fiber volume and will be resisted over a greater part of the failure surface. The first crack behavior is worth considering as the fiber effect was the greatest there in proportion. The first crack load increases by 84% and 132%, respectively, which are both higher than the ultimate load increases, suggesting that the fibers are most effective at the first crack when the crack width is small. This trend is in line with the results of Gouveia et al. [10] who found that the punching resistance and deformation capacity of SFRC flat slabs were increased simultaneously, and with the reduction of crack width at service load reported by Nguyen-Minh et al. [9].

B. Effect of Flexural Reinforcement Ratio (Group 2)

Group 2 clarifies the impact of fiber usage benefits as the specimen with the lowest reinforcement ratio, S4 at 0.725%, cracked at 40.00 kN, which is well above the control, but the ultimate load of 64.67 kN was essentially the same as that of S1. It also exhibited the greatest central deflection of the group (10.30 mm) and very high tensile strain in the reinforcement. As the ratio rose to 1.035% in S5 and 1.346% in S6/S2, the ultimate load increased to 80.72 and 85.19 kN, as Figure 4 and Table 3 show.

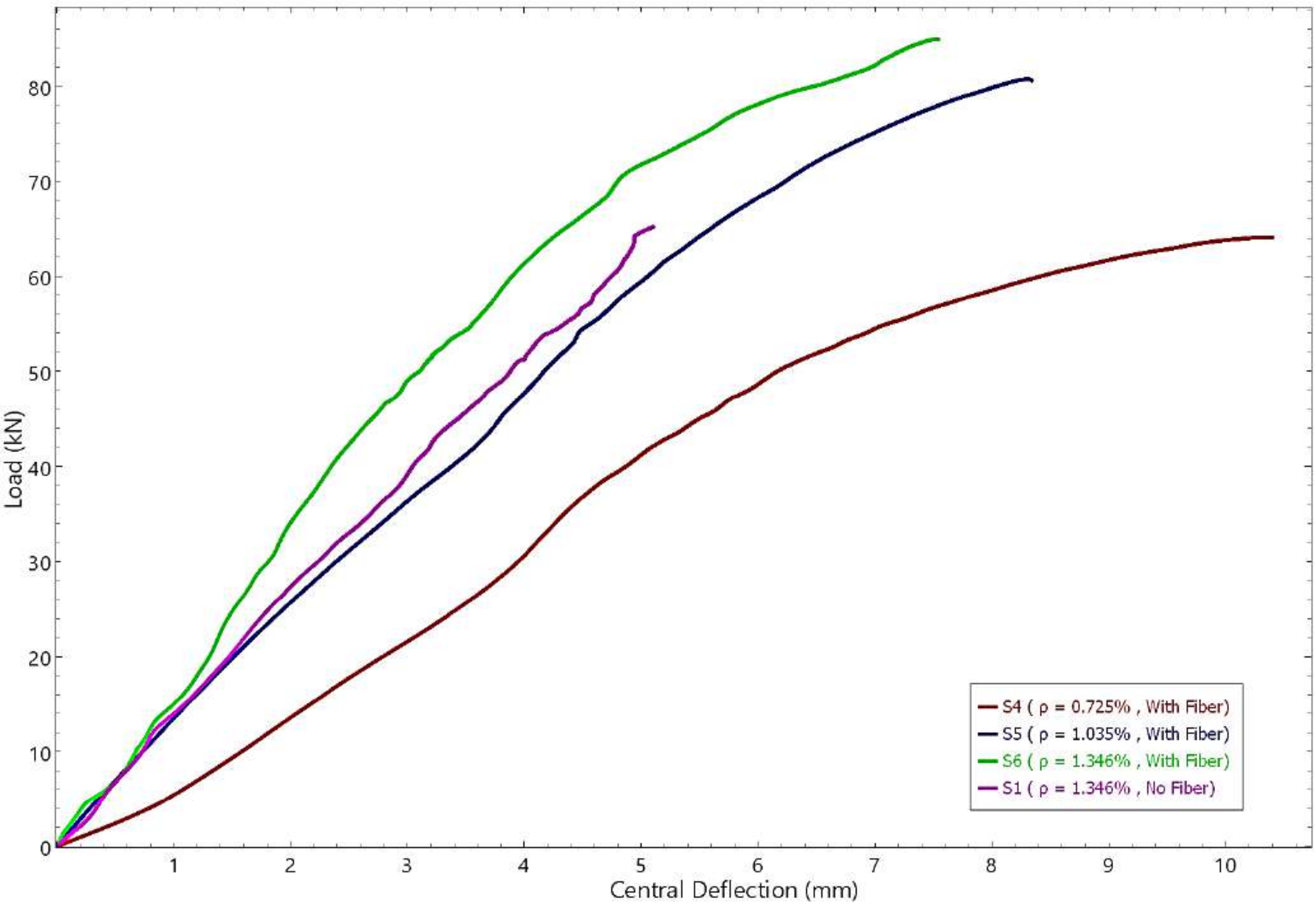

Figure 4: Load versus central deflection, Group 2 (effect of reinforcement ratio).

Table 3: Critical loads and central deflections, Group 2 (effect of reinforcement ratio)

Slab	Stage	Load (kN)	Central deflection (mm)
S1	First crack	25.00	1.82
	Ultimate	65.11	5.10
S4	First crack	40.00	4.48
	Ultimate	64.67	10.30
S5	First crack	37.00	3.06
	Ultimate	80.72	8.30
S6/S2	First crack	46.00	2.77
	Ultimate	85.19	7.53

The difference between S4 and S6/S2 indicates that SFRC is not a complete solution to the problem of insufficient flexural reinforcement. The fibers are used for crack control and post-cracking resistance, and the flexural bars are used to provide the main tensile force that the slab needs to create a stable punching mechanism and mobilize the compression strut around the column. If the ratio is low, the slab yields and deforms significantly before the punching capacity is attained and the response is more like a flexure-influenced limit, but a cone is still formed. This behavior is in line with Teng et al. [5] who emphasized that the reinforcement ratio is a first order parameter that controls the punching strength and that low reinforcement ratios can lead to high yielding before punching, and with the observation by Mabrouk et al. [6] that the flexural reinforcement ratio has a first order effect on capacity and deformation. This reading is supported by the secant stiffness data. The load-deformation gradient of the lightly reinforced S4 was the lowest of the group, thus confirming that the reduction in reinforcement, and not any difference in fiber content, controlled the load-deformation gradient.

C. *Effect of SFRC Zone Size (Group 3)*

Group 3 confirms that the lateral spread of the fibers is as important as the fibers themselves. The smallest fibered zone, C+d in S7, resulted in a slight increase in the ultimate load to 70.66 kN and a ductility index of 1.23, which is essentially the same as the plain control. The C+2d zone in S8 resulted in an ultimate load of 74.57 kN, and the widest C+3d zone in S9 had an ultimate load of 84.45 kN with a much larger deformation capacity as shown in Figure 5 and Table 4. The trend is explained by the cone measurements. S7 had a localized failure and the highest average failure angle of the entire program, 36.10 degrees, which means that the inclined surface soon left the narrow fibered region and crossed the plain concrete for most of its length. The wider crack fields of S8 and S9 were due to the critical crack having to pass through a larger fibered area before reaching the tension face.

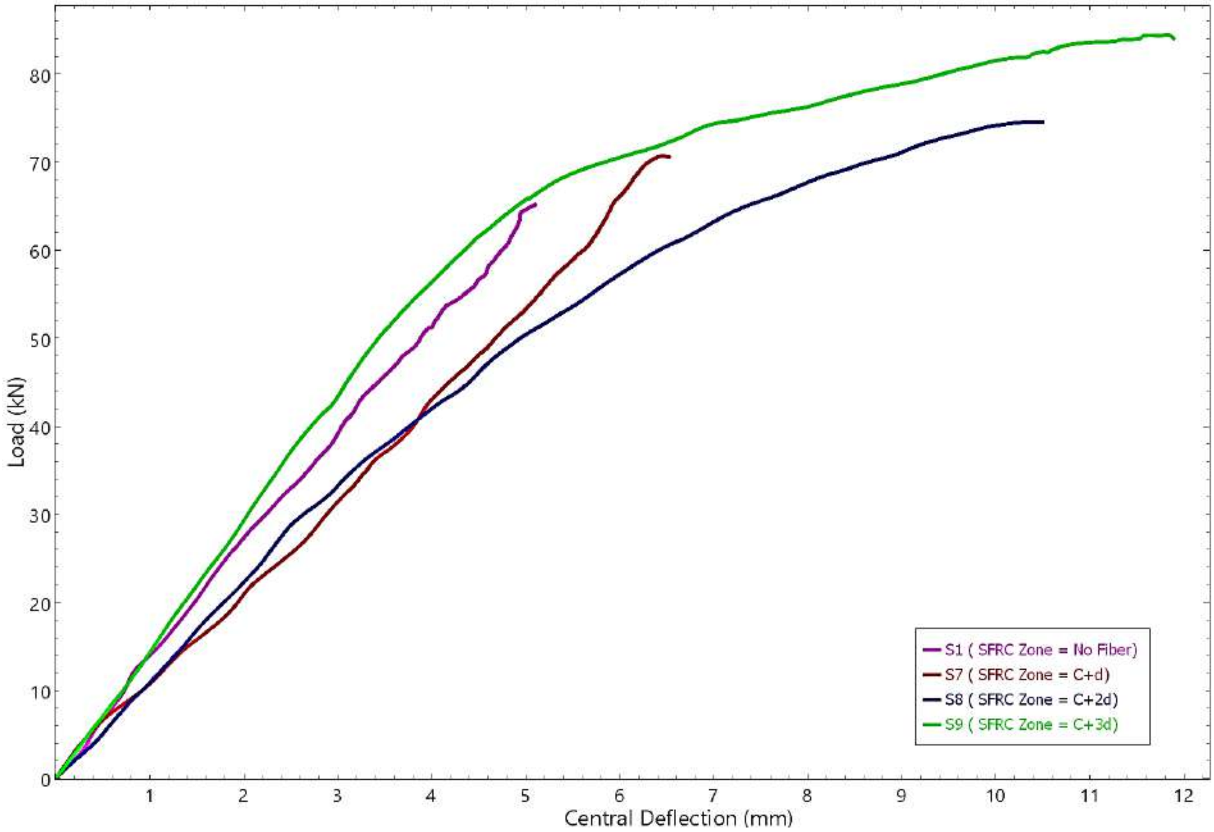

Figure 5: Load versus central deflection, Group 3 (effect of SFRC zone size).

Table 4: Critical loads and central deflections, Group 3 (effect of SFRC zone size)

Slab	Stage	Load (kN)	Central deflection (mm)
S1	First crack	25.00	1.82
	Ultimate	65.11	5.10
S7	First crack	32.00	3.04
	Ultimate	70.66	6.46
S8	First crack	42.00	3.90
	Ultimate	74.57	10.42
S9	First crack	39.00	2.60
	Ultimate	84.45	11.82

This means that there is a minimum fibered zone, in the geometry tested, below which the use of targeted fiber placement is not beneficial because the failure surface simply avoids the fibers, between C+d and C+2d. After that threshold, increasing the size of the zone further increases the deformation capacity. The cone geometry was used to provide an independent confirmation, since the average failure angle was reduced from 36.10 degrees in S7 to 22.87 and 24.41 degrees in S8 and S9, respectively, and the cone area was increased when the zone was larger than C+d. This is consistent with the results of Abdel-Rahman et al. [7] who found that the larger the fibered region around the column, the better the punching response and the further the critical failure plane was moved away from the column face, and it is compatible with the critical shear crack concept used by Gouveia et al. [8].

D. Effect of Load Eccentricity (Group 4)

Group 4 results presented an opposite trend compared to Group 3 as the benefit of SFRC was greatly reduced as the load eccentricity increased. The concentric SFRC reference S10/S2 reached 85.19 kN, while S11 with an eccentricity ratio of 0.5 failed at 60.03 kN and S12 with an eccentricity ratio of 1.0 failed at only 25.73 kN. The first crack load decreased even more rapidly, from 46.00 kN to 16.00 kN and then to 9.50 kN as illustrated in Figure 6 and Table 5. The crack pattern evolved in parallel: in S10/S2, the crack pattern was an almost symmetric cone; in S11, the crack pattern was an asymmetric crack field on the high eccentricity side; and in S12, the crack pattern was a one-way flexural failure with no measurable punching cone.

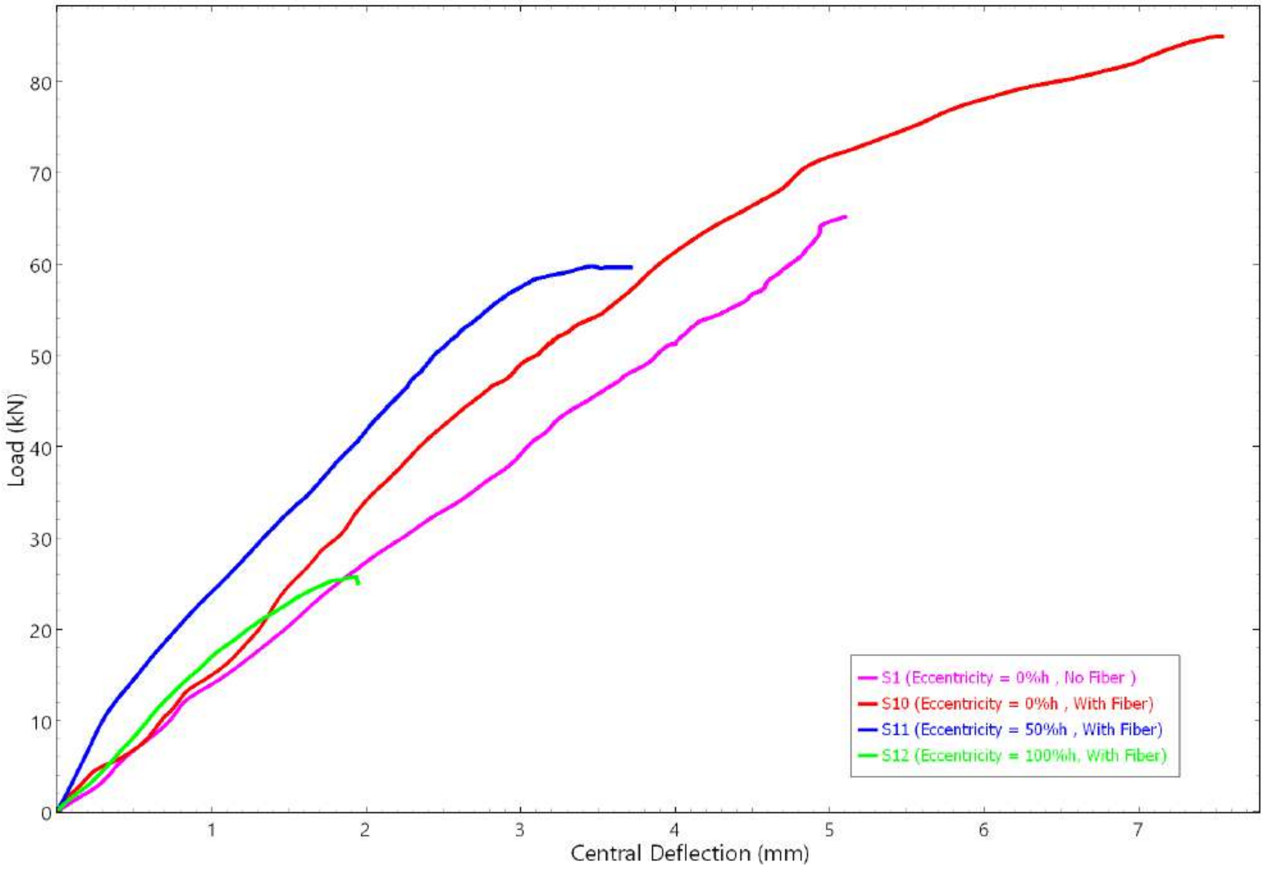

Figure 6: Load versus central deflection, Group 4 (effect of load eccentricity).

Table 5: Critical loads and central deflections, Group 4 (effect of load eccentricity)

Slab	Stage	Load (kN)	Central deflection (mm)
S1	First crack	25.00	1.82
	Ultimate	65.11	5.10
S10/S2	First crack	46.00	2.77
	Ultimate	85.19	7.53
S11	First crack	16.00	0.57
	Ultimate	60.03	3.81
S12	First crack	9.50	0.56
	Ultimate	25.73	1.93

Eccentric loading introduces an unbalanced moment to the shear force, which increases the total stress, and results in higher tensile stress on one side of the column and lower tensile stress or even a net compressive stress on the other side of the column. The higher the eccentricity, the more the moment-induced stress on the critical side dominates, the less the shear perimeter is used, and the less capacity the connection has. The progressive loss of capacity is in line with the findings of Abdel-Rahman et al. [7] who found that even when fibers are present, the capacity of punching is degraded with eccentric loading, while the shift towards a flexure controlled response is in line with the findings of Tan and Venkateshwaran [11]. The most important finding is that S12 changed to a flexural failure, meaning that the punching cone that the fibers are supposed to toughen was not formed at all. The deformation data contributes to the concern. The central deflection at failure was decreased from 7.53 mm for the concentric reference to 3.81 mm for S11 and 1.93 mm for S12, and the eccentric slabs were able to carry much less load and failed at a much smaller deflection. This is one of the main benefits of SFRC under concentric loading which was largely eliminated under high eccentricity, which is in line with the findings of Deifalla [3] that combined shear and moment is much more complicated than concentric punching and that eccentricity is the most detrimental of the five parameters studied.

E. Effect of Fiber Volume Fraction (Group 5)

The most direct evidence of the effect of the fiber dosage on the cracking threshold and ultimate resistance is provided by Group 5. Raising the dosage from 0 to 0.5, 1.0, and 1.5% lifted the ultimate load from 65.11 kN to 76.25, 85.19, and 112.16 kN, while the first crack load rose from 25.00 kN to 34.00, 46.00, and 48.00 kN, as Table 6 summarizes. The increase at the highest dosage was significant and the ultimate strength was about 72% higher than the plain control and the highest capacity recorded during the entire program. The strains recorded indicate that the higher fiber content enabled the slab to sustain a much higher reinforcement strain before failure, with S15 reaching about 6850 microstrain at ultimate load, well beyond yield.

Table 6: Critical loads and central deflections, Group 5 (effect of fiber volume fraction)

Slab	Stage	Load (kN)	Central deflection (mm)
S1	First crack	25.00	1.82
	Ultimate	65.11	5.10
S13	First crack	34.00	1.25
	Ultimate	76.25	6.48
S14/S2	First crack	46.00	2.77
	Ultimate	85.19	7.53
S15	First crack	48.00	3.35
	Ultimate	112.16	8.95

It is important to note here that the strength trend is different from the ductility trend. The ultimate load kept rising steadily without any sign of saturation up to 1.5%, and the ductility index rose marginally between 1.0 and 1.5% (from 1.61 to 1.58), within the experimental scatter. A dosage of about 1.0% therefore provides the maximum advantage of deformation capacity for the geometry tested, and further increases only lead to an increase in the peak load. These strength results are similar to those of Gouveia et al. (2014) who reported an increase of about 64% in the maximum punching capacity at the higher fiber dosages used, and to those of Nguyen-Minh et al. (2011) who showed that fibers change the failure mode from sudden and brittle to more ductile. The first crack load was again increased by 92% at the 1.5% dosage, which was greater than the proportional increase in the ultimate load, and was similar to the trend observed in Group 1, where fibers were most effective at the first crack. The higher the cracking threshold, the better for serviceability because the less cracking and the narrower the crack widths under service load, the better it will be for durability as less moisture and aggressive agents will be able to enter the structure.

F. Punching Cone Geometry

The cone on the tension face was traced to give an independent confirmation of the fiber mechanisms. In general, the SFRC slabs had shallower cone angles and larger cone areas than the plain control, which means that the failure surface was spread out over a greater horizontal distance and absorbed more energy. The cone area measured was found to be greater in the highest dosage slab (S15) with 161,690 mm² compared to 101,427 mm² in S1, while the cone perimeter was always longer for the fibered specimens. The average punching cone angle for the program was 24.67 degrees, narrow-zone S7 was 36.10 degrees and eccentric S11 was 18.34 degrees. The traced cones for the three fiber-height specimens are shown in Figure 7 and the average cone angle for each specimen is summarized in Figure 8. Many previous studies reported load and deflection without correlating to the measured failure surface; one of the more novel aspects of the program is the relationship between cone geometry, fibered zone size, and structural response [8], [7].

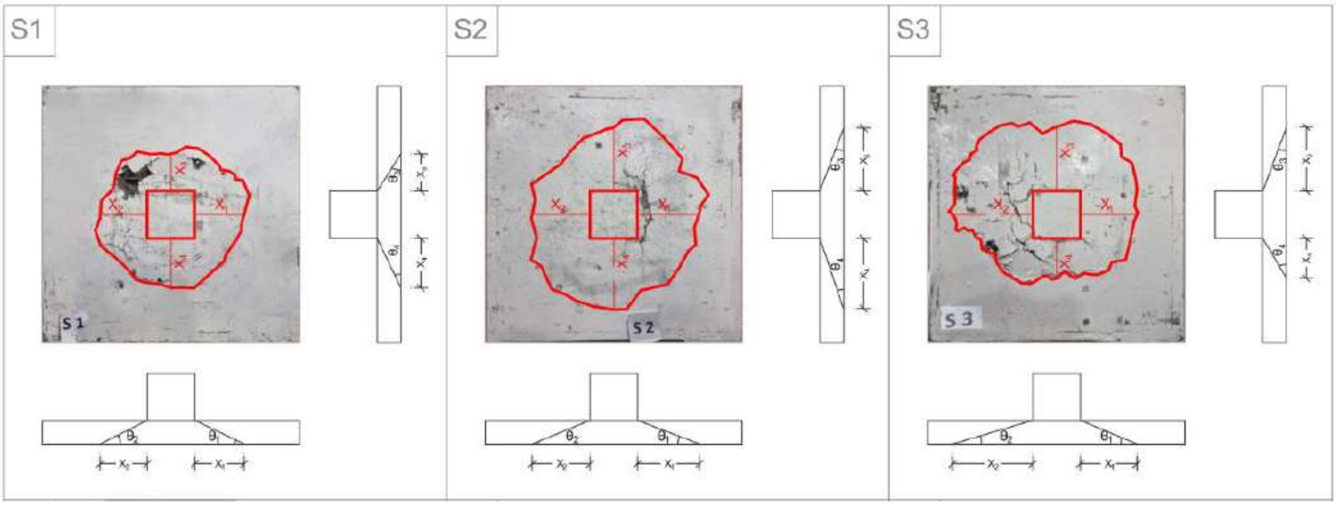

Figure 7: Traced punching cone geometry and measured failure angles, Group 1 (S1, S2, S3).

Table 7: Cone geometry and average failure angles for representative specimens

Slab	Cone area (mm²)	Cone perimeter (mm)	Avg. angle (°)	Failure mode
S1	101,427	1,194	27.61	Punching
S3	150,192	1,550	22.51	Punching
S7	70,365	1,052	36.10	Punching
S9	136,161	1,502	24.41	Punching
S11	147,473	1,171	18.34	Punching
S12	0 (no cone)	0	—	Flexural
S15	161,690	1,454	19.61	Punching

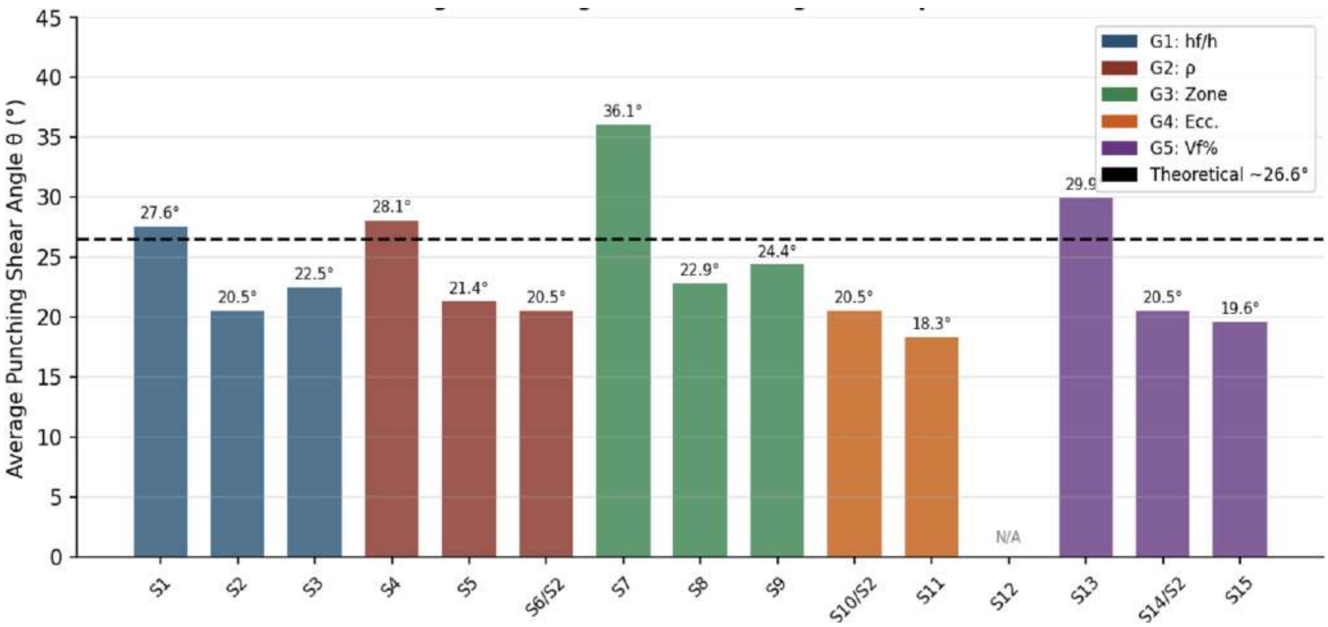

Figure 8: Average punching shear cone angle for all specimens, grouped by parameter.

G. Ductility and Stiffness

The deformation capacity was summarized by a ductility index (ratio of the ultimate deflection to the yield deflection) and a secant stiffness. For all specimens, both indices are plotted together in Figure 9. The ductility index was found to be significantly higher with the increase in fiber height ratio, ranging from 1.26 in S1 to 1.61 in S2 and 2.67 in S3, the highest in the program, while the secant stiffness decreased from 12.77 to 7.12 kN/mm for the same specimens. This inverse pairing is a reflection of the change from a brittle sudden failure to a gradual energy dissipating failure. This is also true in Group 3, where the ductility index of the narrow-zone S7 was 1.23, and that of the wide-zone S9 was 2.24. A word of caution is needed for the eccentric specimens. Their ductility index was between 1.45 and 1.58, which appears to be stable, but that index is a ratio of deflections which were themselves drastically reduced. The eccentric indices should not be interpreted in isolation; an index of 1.45 on an ultimate deflection of 1.93 mm is a much more brittle reality than the same index on 7.53 mm.

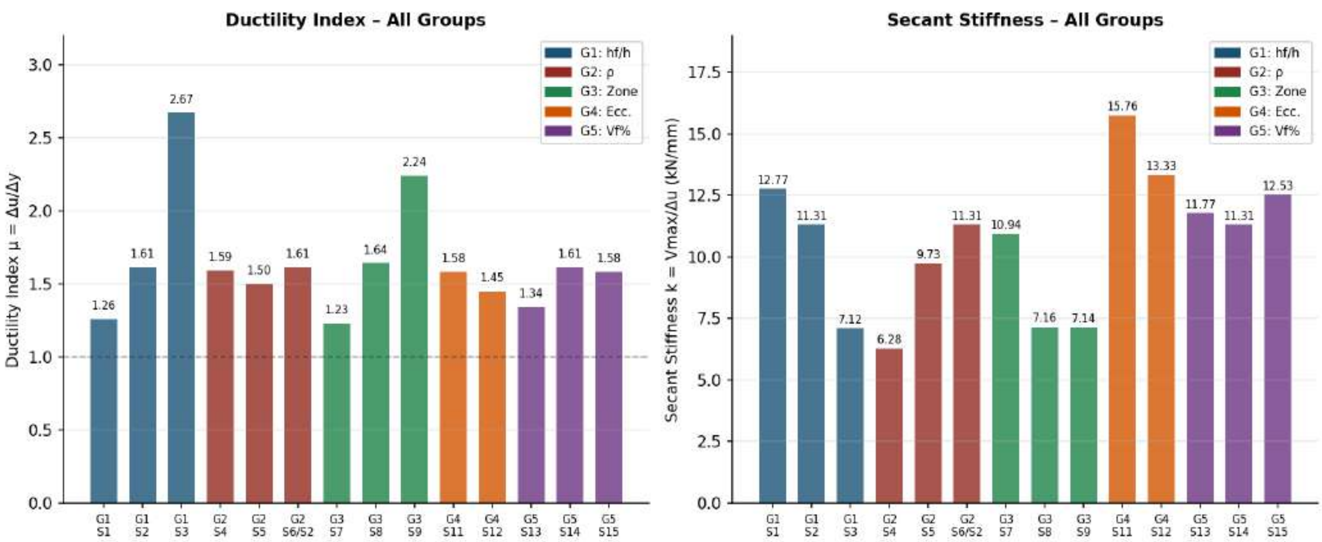

Figure 9: Ductility index and secant stiffness for all tested specimens.

H. Comparison with ACI 318 Predictions

The measured capacities were compared with the punching strength predicted by a two-layer application of the ACI 318 concrete contribution, where the normal concrete and SFRC layers were each given their own concrete contribution over their respective depths [12]. For all concentric specimens, the measured strength exceeded the ACI prediction and the code was conservative throughout. However, the conservatism was progressive as the influence of the fiber contribution grew. The experimental-to-predicted ratio ranged from 1.43 for the plain control to 1.83 for the two-layer slab and 1.96 for the full-depth slab in Group 1 and from 1.43 at zero fiber to 2.44 at 1.5% in Group 5. The answer is simple. The ACI concrete equation is essentially based on the concrete strength, the effective depth and the critical perimeter and does not explicitly consider the residual tensile strength and crack-bridging effect of the fibers. This is the reason why the predicted capacity in

Group 5 was almost constant at 46 kN and the measured capacity increased from 65.11 to 112.16 kN. This limitation has been reported by Ju et al. [2] who stated that the design criteria for SFRC punching are still not clear and by Deifalla [3] who pointed out that there is still a lack of agreement between the punching provisions when fibers or combined actions are considered.

The comparison should not be interpreted as a comfortable safety margin. In a few instances the prediction was close to the test result, but not for good modeling reasons. In Group 3, the ACI prediction was the same for S7, S8 and S9, while the measured capacities were seen to increase with the fibered zone, and the constant prediction completely missed the beneficial zone-size effect and treated three physically different specimens as the same. The same applies to S12, which has a good experimental-to-predicted ratio, but is coincidental as S12 did not form a cone at all and failed in flexure at high eccentricity. The experimental capacities and the ACI predictions for the concentric specimens are shown in Table 8.

Table 8: Experimental capacity versus ACI 318 prediction (concentric specimens)

Slab	First crack (kN)	Vmax (kN)	ACI Vcal (kN)	Vexp/Vcal
S1	25.0	65.11	45.60	1.43
S2	46.0	85.19	46.44	1.83
S3	58.0	95.16	48.56	1.96
S4	40.0	64.67	46.84	1.38
S5	37.0	80.72	46.84	1.72
S7	32.0	70.66	48.96	1.44
S8	42.0	74.57	48.96	1.52
S9	39.0	84.45	48.96	1.72
S13	34.0	76.25	45.39	1.68
S15	48.0	112.16	46.05	2.44

The trend of the five groups is consistent in terms of punching behavior of the slab-column connections of layered NC-SFRC. The fiber height ratio and the fiber volume fraction were the most effective parameters to improve both strength and deformation capacity under concentric loading, and the through-depth position of the fibers was a design parameter in its own right, not a by-product of total fiber content. The cone geometry indicated that the size of the fibered zone was beneficial only if it was sufficiently large to intercept the developing failure surface. The flexural reinforcement ratio was used to determine the maximum strength that the fibers could mobilize, which showed that fibers and conventional reinforcement are complementary and not interchangeable. However, load eccentricity affected the mechanism that the fibers are supposed to toughen and decreased strength and deformation capacity, which ultimately altered the failure mode. The ACI predictions were always conservative for the concentric specimens, but did not consider the contribution of the fibers, the zone-size effect or the eccentric failure mode, which is consistent with the findings of Einpaul et al. [4] who concluded that the modelling of the key parameters is important for punching predictions. A more rational design approach for these systems would have to take into account the residual tensile contribution of the SFRC, the vertical position of the fibered layer, the lateral size of the fibered zone, the reinforcement ratio, and the moment transfer due to any eccentricity.

IV. CONCLUSIONS

In this study, the punching shear behaviour of fifteen two-layer slab-column connections with normal concrete and steel fiber reinforced concrete was investigated experimentally in five parametric groups. The following are the main conclusions.

- The punching performance was significantly improved by replacing the tension half of the slab with SFRC. The two-layer slab failed at 85.19 kN and cracked at 46.00 kN, compared to 65.11 and 25.00 kN for the plain control, respectively, representing increases of approximately 84% and 31% in the ultimate load and first crack load, respectively. These were increased to approximately 46% and 132% by the full-depth slab. The fiber effect was greatest at the beginning of cracking.
- The position of the SFRC layer in the through-depth direction is an independent design parameter. The full-depth benefit was captured to a large extent by placing fibers only in the tension half, since this is where flexural cracking begins and where crack bridging is most effective. A designer can thus limit the use of the more costly fibered concrete to the tension half and the compression half to conventional concrete.
- The ultimate load that the fibers could mobilize was controlled by the flexural reinforcement ratio. The lightly reinforced slab cracked early but failed at essentially the control capacity while deflecting the most in its group. SFRC cannot make up for lack of flexural reinforcement, and a minimum ratio must be maintained if the strength benefit is to be manifested and not hidden by premature yielding.
- The lateral extent of the fibered zone was of assistance only when it was sufficiently large to intercept the developing failure surface. The narrowest zone, C+d, provided virtually no improvement and resulted in the highest cone angle in the program, and increasing the zone to C+2d and C+3d increased both strength and ductility. For the geometry tested, there is a minimum fibered zone between C+d and C+2d.
- Load eccentricity was the most harmful parameter. Compared to the concentric SFRC slab, the ultimate load decreased to 60.03 kN at an eccentricity ratio of 0.5 and 25.73 kN at an eccentricity ratio of 1.0, the central deflection at failure reduced significantly and the failure mode changed from a symmetric cone to an asymmetric field and then to a one-way flexural failure. Eccentric connections need explicit consideration of the moment-shear interaction rather than reliance on the fiber toughening alone.
- The fiber volume fraction increased the cracking threshold and the ultimate load, reaching 112.16 kN at 1.5%, which is approximately 72% higher than the control. However, the ductility index did not change significantly between 1.0 and 1.5%, and a dosage close to 1.0% would provide most of the benefit of increased

deformation capacity with higher dosages primarily increasing the peak load.

- For all concentric specimens, the ACI 318 predictions were conservative, and the conservatism increased with the amount of fiber contribution, since there is no direct fiber term in the code. The predictions also did not reflect the zone-size effect and the eccentric failure mode, indicating the need for a fiber contribution term in future punching provisions for hybrid SFRC flat-slab connections.

In general, the experimental results have shown that the two-layer system of normal concrete and steel fiber reinforced concrete is a feasible method to enhance the punching capacity of flat slab-column connections, if the fibers are located at the critical crack zones. Future work should be extended to full-scale connections, investigate the long-term behavior of the layer interface, investigate the eccentric case in greater detail, and aid in the development of a design model that directly considers the residual tensile contribution of the SFRC.

CONFLICTS OF INTEREST

The authors declare that they have no conflicts of interest.

ACKNOWLEDGMENT

The authors gratefully acknowledge the support of the Department of Civil Engineering, Gaziantep University, in carrying out the experimental program.

REFERENCES

[1] A. Silva, M. G. Marques, L. M. Trautwein, R. B. Gomes, and G. N. Guimarães, "Punching of reinforced concrete flat slabs with holes and shear reinforcement," *REM - International Engineering Journal*, vol. 70, no. 4, pp. 407–413, 2017. Available from: https://doi.org/10.1590/0370-44672017700022

[2] H. Ju, N.-R. Cheon, D. H. Lee, J.-Y. Oh, J.-H. Hwang, and K. S. Kim, "Consideration on punching shear strength of steel-fiber-reinforced concrete slabs," *Advances in Mechanical Engineering*, vol. 7, no. 5, pp. 1–14, 2015. Available from: https://doi.org/10.1177/1687814015584251

[3] Deifalla, "A mechanical model for concrete slabs subjected to combined punching shear and in-plane tensile forces," *Engineering Structures*, vol. 231, p. 111787, 2021. Available from: https://doi.org/10.1016/j.engstruct.2020.111787

[4] Einpaul, J. Bujnak, M. Fernández Ruiz, and A. Muttoni, "Study on influence of column size and slab slenderness on punching strength," *ACI Structural Journal*, vol. 113, no. 1, pp. 135–145, 2016. Available from: https://doi.org/10.14359/51687945

[5] S. Teng, K. Chanthabouala, D. T. Y. Lim, and R. Hidayat, "Punching shear strength of slabs and influence of low reinforcement ratio," *ACI Structural Journal*, vol. 115, no. 1, pp. 139–150, 2018. Available from: https://dr.ntu.edu.sg/entities/publication/2e03bcdf-ffcc-417e-aa89-7cf020d017ed

[6] R. T. Mabrouk, A. Bakr, and H. Abdalla, "Effect of flexural and shear reinforcement on the punching behavior of reinforced concrete flat slabs," *Alexandria Engineering Journal*, vol. 56, no. 4, pp. 591–599, 2017. Available from: https://doi.org/10.1016/j.aej.2017.05.019

[7] M. Abdel-Rahman, N. Z. Hassan, and A. M. Soliman, "Punching shear behavior of reinforced concrete slabs using steel fibers in the mix," *HBRC Journal*, vol. 14, no. 3, pp. 272–281, 2018. Available from: https://doi.org/10.1016/j.hbrcj.2016.11.001

[8] N. D. Gouveia, M. Lapi, M. Orlando, D. M. Faria, and A. M. P. Ramos, "Experimental and theoretical evaluation of punching strength of steel fiber reinforced concrete slabs," *Structural Concrete*, vol. 19, no. 1, pp. 217–229, 2018. Available from: https://doi.org/10.1002/suco.201700136

[9] Nguyen-Minh, M. Rovňák, T. Tran-Quoc, and K. Nguyenkim, "Punching shear resistance of steel fiber reinforced concrete flat slabs," *Procedia Engineering*, vol. 14, pp. 1830–1837, 2011. Available from: https://doi.org/10.1016/j.proeng.2011.07.230

[10] N. D. Gouveia, N. A. Fernandes, D. M. Faria, A. M. Ramos, and V. J. Lúcio, "SFRC flat slabs punching behaviour: Experimental research," *Composites Part B: Engineering*, vol. 63, pp. 161–171, 2014. Available from: https://doi.org/10.1016/j.compositesb.2014.04.005

[11] Tan and A. Venkateshwaran, "Punching shear in steel fibre reinforced concrete slabs without traditional reinforcement," *IOP Conference Series: Materials Science and Engineering*, vol. 216, p. 012014, 2017. Available from: https://doi.org/10.1088/1757-899X/246/1/012025

[12] ACI Committee 318, *Building Code Requirements for Structural Concrete (ACI 318-25) and Commentary*. Farmington Hills, MI: American Concrete Institute, 2025. Available from: https://tinyurl.com/3vcvk28e